Small Prototype Gamma Spectrometer Using CsI(Tl) Scintillator Coupled to a Solid-State Photomultiplier

Eric M. Becker, *Member IEEE*, Abdollah T. Farsoni, *Member, IEEE*, Abdulsalam M. Alhawsawi, *Member, IEEE*, and Bemnet Alemayehu, *Member, IEEE*

***Abstract*— Small solid-state photomultipliers (SSPMs) are an alternative scintillator light-detection technology to traditional photomultiplier tubes that offer advantages such as lower bias voltages and insensitivity to magnetic fields. A digital spectrometer using a commercially available SSPM was constructed and characterized at Oregon State University as a prototype for small, highly-mobile, low-power, robust spectroscopy devices. The SSPM has over 19,000 microcells in a photo-sensitive area of 6.32 x 6.32 mm and was coupled to 6 x 6 x 10 mm reflectively-coated CsI(Tl) crystals. The rest of the spectrometer consists of a fast preamplifier and 200 MHz, 12-bit digital pulse processor based around a field-programmable gate array (FPGA). The efficiency, resolution, linearity, and peak-to-Compton ratio of the system were characterized.**

***Index Terms*—digital pulse processing, solid-state photomultiplier, gamma radiation detection, scintillation**

I. Introduction

SOLID-STATE photomultipliers (SSPMs) are the result of a progression toward smaller, more robust photo-sensor technology that started in the 1960's with the development of the avalanche photodiode (APD) [1]. An SSPM typically consists of several thousand microcells, each encompassing an APD and quench resistor and operating in the Geiger region of voltage-bias response. When scintillation photons are incident on the SSPM, each one is ideally absorbed by a different microcell, each of which then discharges, all individually generating a current pulse of the same magnitude. The microcells are all connected to one output anode and thus generate a current pulse proportional to the number of microcells that discharge. Thus, the output signal will be proportional to the number of microcells that absorbed photons and in turn proportional to the energy of the radiation interaction event [1]-[3].

Current iterations of SSPM technology have sufficient dynamic range and resolution to be used as radiation detectors able to perform energy spectroscopy comparable to that of the more common photomultiplier tube (PMT) [4], [5], and [6]. SSPMs have several advantages over PMTs which include insensitivity to magnetic fields, compact size, lower cathode voltage bias, and increased durability. Like PMTs, SSPMs typically have an internal gain factor of 10^6, a fast rise time, and allow for single-photon discrimination [1]-[5].

PIN diodes are another solid-state photo-multiplication technology. Based in part on the familiar PN-junction diode, PIN diodes have an intrinsic ("I") region between the P and N regions. Despite having lower levels of noise than simpler PN diodes, they are often still cooled in order to be sensitive to lower energies [7]. When not cooled, PIN diodes have much worse resolution than SSPMs and PMTs because they are only sensitive to larger amounts of charge to overcome the inherent noise [8], [9]. For these reasons, although PIN diodes share some of the same advantages over PMTs that SSPMs do, a PIN diode array was not chosen for this device.

For the reasons above, along with higher economic viability via mass-production, SSPMs would provide superior capabilities for applications such as radiological event response, on-site treaty verification, and remote or personal radiation monitoring, all of which require a small, mobile, rugged, low-power device or network of devices able to perform radiation energy spectroscopy, radioisotope identification, or dose measurement.

The purpose of this study is to characterize a prototype gamma radiation spectrometer that incorporates an SSPM coupled to a scintillation crystal and a digital pulse processor (DPP). The SSPM and DPP are both integral to this device since the design goal is for the spectrometer system to be easily miniaturized and able to perform a variety of functions in the field.

II. Device and Setup

A. Front-end components

The spectrometer used in this study essentially consists of two parts: the radiation sensor and the DPP. The radiation sensor is comprised of the scintillation crystal, SSPM, casing, and preamplifier.

Manuscript received June 15, 2012.

The authors are with the Oregon State University, Corvallis, OR 97331 USA (e-mail: beckere@onid.orst.edu, tavakola@onid.orst.edu, alhawsaa@onid.orst.edu, alemayeb@onid.orst.edu).

The type of SSPM used in this study was manufactured by SensL and features a sensor area composed of four 3.05 x 3.05 mm photo-sensitive pads. Each of the smaller photo-sensitive regions possesses 4,774 microcells, making the total number of microcells on the SSPM 19,096. The fill-factor for each of the photo-sensitive pads is 65%. However, the four pads are separated from each other by 0.25 mm of non-sensitive area. The calculation of total fill-factor is a ratio of photo-sensitive area to total sensor area in the form of

$$FF_{total} = \frac{(L \cdot W) \cdot ff}{L \cdot (W + w) + (w^2)}, \quad (1)$$

where FF_{total} is the total fill-factor, L is the length of one photo-sensitive pad, W is the width of one photo-sensitive pad, ff is the pixel fill-factor for one of the four pads, and w is the width between the pads. For this device, L and W are 3.05 mm, w is 0.25 mm, and ff is 65% [10]. This yields a total fill-factor (FF_{total}) of 60%.

The overall device is 10.10 x 8.90 x 2.00 mm, which does not include the length of the anode and cathode pins, which are non-essential dimensions [10]. The SSPM was operated at -30.0 V for all measurements.

The CsI(Tl) crystal used in this study was manufactured by Hilger Crystals. CsI(Tl) was chosen as the scintillation material for this spectrometer because of its relatively high gamma ray absorption efficiency and because its peak light output wavelength of 550 nm was most ideally suited to the peak wavelength sensitivity of the SSPM, which is 500 nm [10].

Fig. 1. One of the SSPMs and CsI(Tl) crystals used in the measurements. The crystals were purchased with the reflective epoxy coating.

The CsI(Tl) crystals used were 6 x 6 x 10 mm with a reflective white epoxy coating on all sides except one of the 6 x 6 mm faces. An SSPM and CsI(Tl) crystal are shown in Fig. 1. The epoxy on one of the CsI(Tl) crystals was later removed and the crystal was wrapped with Teflon tape. The crystals were coupled optically via BC-630 silicone grease, centered above the photosensitive area of the SSPM. This assembly was then wrapped with Teflon to ensure light reflectivity at the edges of the device. To block light sources other than the CsI(Tl) crystal, a custom light shield was constructed from molded plastic and black electrical tape and fitted over the assembly. The effectiveness of the light shield was verified by monitoring the assembly via oscilloscope with ambient lighting on and off.

Two different assemblies were constructed. Assembly 1-$C1_{epoxy}$ consisted of SSPM 1 and epoxy-coated crystal $C1_{expoy}$. Assembly 2-$C2_{epoxy}$ consisted of SSPM 2 and epoxy-coated crystal $C2_{epoxy}$. Assembly 2-$C2_{Teflon}$ consisted of SSPM 2 and crystal $C2_{epoxy}$ with the epoxy removed via sanding with sandpaper (600-grit) The crystal was then polished with denatured ethanol and wrapped with four layers of Teflon [11], which provided internal scintillation light reflection, opacity to external light in addition to the custom light shield mentioned above, and the mechanism by which the crystal was secured in place. Measurements were made with assembly 2-$C2_{epoxy}$ and 2-$C2_{Teflon}$ to assess the effectiveness of different reflective materials.

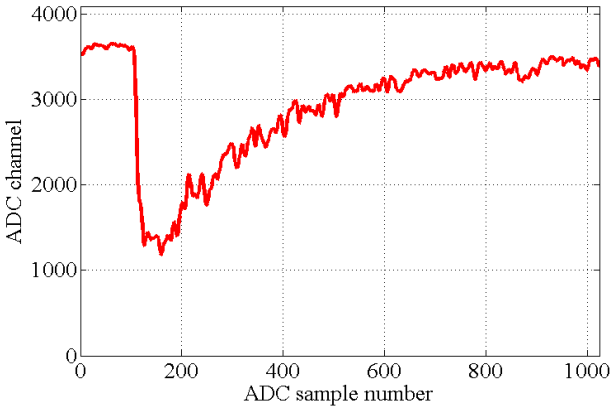

Fig. 2. Example of a pulse waveform from the spectrometer viewed in the MATLAB user interface.

The assemblies were individually connected to an evaluation board (EVB), which housed the preamplifier. The preamplifier employed an OPA656 FET-input operational amplifier with ultra-low (7nV/√Hz) input voltage noise to achieve a very low integrated noise in wideband photodiode transimpedance applications [12]. The time constant for this preamplifier was short enough that it functioned as a non-integrating preamplifier for the CsI(Tl) crystal. The feedback resistance and capacitance were designed to provide 470x gain for the SSPM used, providing a total range of 2 V over the dynamic range of the SSPM. Power to the EVB was provided by a wall-plug, transformed on the board to ±6.5 V component power and the -30.0 V bias voltages for the SSPM [13].

B. Back-end components

The EVB preamplifier output was connected to the DPP input via SMA-to-SMA cable. The DPP is an FPGA-based RX1200-D produced by Avicenna Instruments, LLC, which has an ADC with 12-bit resolution, and a sampling rate of 200 MHz [14]. Our DPP has a custom FPGA firmware with both an oscilloscope and multi-channel analyzer (MCA) mode and uses a MATLAB algorithm to control the FPGA functions from a host computer. This algorithm allows the user to toggle between modes and set other parameters, such as input-offset, ADC-offset, trigger threshold, conversion gain, and integration time. In oscilloscope mode, the digital pulse waveforms are displayed in MATLAB as a sequence of 1024 samples, as seen in Fig. 2. When run in MCA mode, the energy histogram is displayed in MATLAB. The FPGA handles all data collection and all pulse processing functions, such as pile-up rejection and energy measurement. To measure the energy deposition in the CsI(Tl) crystal, radiation pulses are integrated over 5000 ns, or 1000 samples. The histogram is implemented using 8 x 18 kb Block RAMS in the FPGA with 4096 channels and a maximum of 32 bits (over four million counts) per channel.

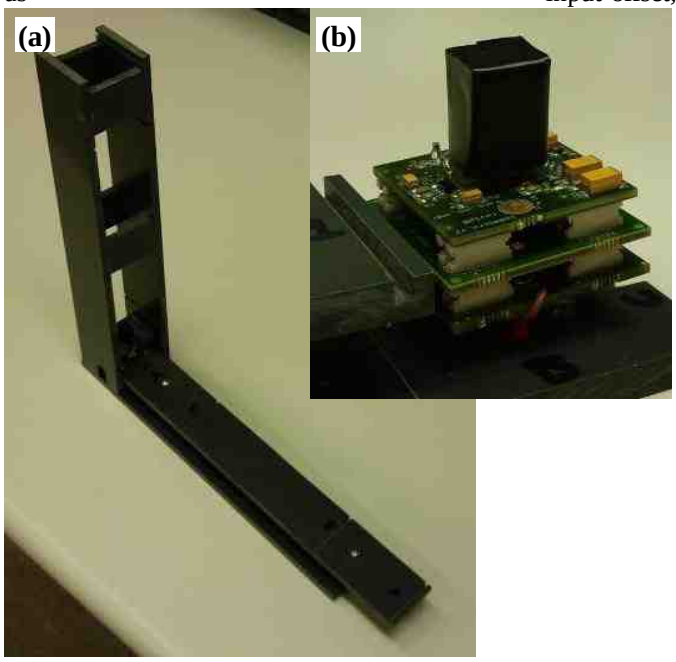

Fig. 3. (a) Test stand with notches cut for insertion of button source-holders and different levels above the detector. (b) Close-up of an assembly (SSPM and CsI(Tl) crystal) in their casing connected to the EVB.

C. Measurement Setup

A custom test stand was constructed from type-II polyvinylchloride (PVC) and is depicted in Fig. 3a. The stand consists of two parts: the plank and the tower. The plank is the horizontal component and also serves as the base for the tower. The EVB was attached to the base of the plank via two screws on the lower board, shown in Fig. 3b. The base also had notches cut out at different horizontal locations away from the detector in which a radiological button-source was held via custom source tray, also made from type-II PVC. The tower is the vertical component of the test stand and was rested directly on top of the base component of the plank. The tower also had notches cut out at different heights away from the detector. The test stand was designed with these notches in mind in order to be able to test close to the detector for energy resolution measurements and further away for photopeak efficiency measurements.

Five isotopes, ^{137}Cs (116 kBq), ^{60}Co (36 kBq), ^{152}Eu (24 kBq), ^{54}Mn (33 kBq), and ^{22}Na (36 kBq), were measured, each in four different positions. In the following descriptions, the 10 mm dimension of the CsI(Tl) crystal was oriented normal to the Earth, as shown in Fig. 3. The first position was “top1”, which held the sources 10.0 mm from the top of the CsI(Tl) crystal for lengthwise energy resolution and linearity measurements. The second position was “top2”, which held the sources 257.0 mm away from the top of the CsI(Tl) crystal for lengthwise efficiency measurements in order to be able to model the sources as points. The third position was “side1”, which held the sources 23.0 mm from the side of the CsI(Tl) crystal for widthwise energy resolution and linearity measurements. The final position was “side2”, which held sources 315.5 mm from the side of the CsI(Tl) crystal for widthwise efficiency measurements, again in order to be able to model the sources as points. For each position of each source, the measurement was ten hours in real-time using the MCA mode of the DPP.

III. Results

A. Energy resolution and linearity

The energy spectra that resulted from the energy resolution measurements with ^{137}Cs are shown in figures 4 and 5. The best full-width half-maximum (FWHM) energy resolution at 662 keV achieved by the spectrometer was 7.88% using assembly 1-$C1_{epoxy}$. The best FWHM energy resolution at 662 keV achieved with assembly 2-$C2_{Teflon}$ was 9.63%. The results for assembly 1-$C1_{epoxy}$ are not far from other published results [5], though they are worse than other known results using similar systems [15]. The results for assembly 2-$C2_{Teflon}$ are significantly worse than expected for this system. However, the previous best resolution of the 662 keV energy peak with the $C2_{epoxy}$ crystal was 10.8% FWHM, so the Teflon coating did improve the reflectivity of the crystal and thus improved the resolution.

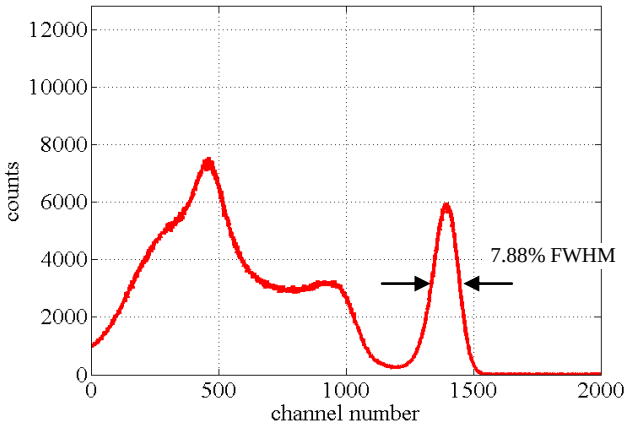

Fig. 4. ^{137}Cs energy spectrum, taken with the source directly above the detector in the "top1" position on the test stand.

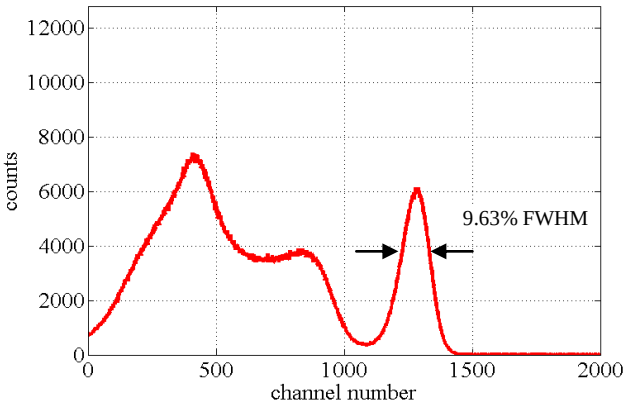

Fig. 5. ^{137}Cs energy spectrum, taken with the source directly above the detector in the "top1" position on the test stand. The assembly used for this measurement was 2-$C2_{Teflon}$.

Both SSPMs used in this spectrometer have specific optimum voltage settings, which were unknown at the time the measurements were taken. The -30.0 V operating condition these SSPMs were placed under for the measurements in this paper was higher than each SSPM's optimal operating voltage. This may have introduced additional noise, and may thus explain why 6.5% FWHM energy resolution at 662 keV was not achieved.

SSPMs, being solid-state devices, are very sensitive to temperature, which strongly affects the dark count rate (noise) [7], [16]. The spectrometer system in this study was unable to be completely thermally stabilized, though efforts were made to maintain a steady temperature, such as starting measurements at the same time of day as well as keeping the system in a facility with a controlled temperature. Despite these efforts, the temperature of the SSPMs may have fluctuated during the measurements. Any fluctuation may also have introduced noise into the system, worsening the energy resolution. Temperature also affects peak position. Thus, when the temperature varies, the ADC channel at which the peak is located may shift during measurement, yielding a worse resolution.

The SSPM signals should also be integrated with a charge-sensitive preamplifier since, again being solid-state devices, their capacitance will change when charge is introduced [17]. The use of the EVB, with the fast (non-charge sensitive) preamplifier, may have introduced error in our measurements since this type of preamplifier does not account for incidences of changing capacitance in solid-state devices.

The large Compton event region of the energy spectra in Figs 4 and 5 is largely due to the small size of the crystal. The peak-to-Compton ratio [18] for assembly 1-$C1_{epoxy}$ for ^{137}Cs was 1.94 for the top1 position, and 1.85 for the side1 position. This is expected since, when measured from the top1 position, a thicker part of CsI(Tl) crystal is presented to the source which would cause multiple Compton events that sum to the photopeak energy to occur more often than from the side1 position.

Figure 6 shows the location of each of the gamma energy peaks in channel number. The trend for the data in this figure is slightly non-linear. Though a polynomial trend line proved to be the best fit available, it still did not quite capture the proper trend of the system. One reason for this phenomenon of non-linearity could be the non-linearity observed in CsI(Tl) crystals [19], [20]. Another possible contribution to this phenomenon for this device is the saturation of the photo-sensitive area of the SSPM at higher energies [21], [16]. Estimating a range of photons incident on the photo-sensitive pixels of 50-90% of the photons generated by radiation interaction with CsI (65,000 photons per MeV [22]), and taking into account the PDE, total fill-factor, and percentage of CsI(Tl) light that is emitted in the 550 nm range (64% [22]), the estimated energy range for which the SSPM will reach saturation is 3.9 to 7.1 MeV.

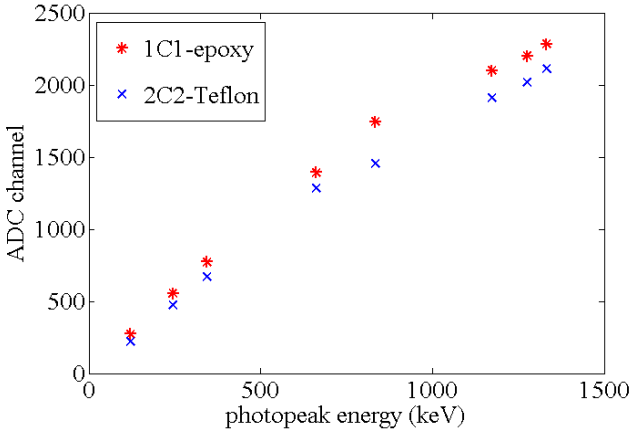

Fig. 6. Energy calibration plot of photopeak energy centroid versus ADC channel number for assemblies 1- $C1_{epoxy}$ and 2- $C2_{Teflon}$, measured from the top 1 position. Error bars are within the size of the data points.

Figure 7 shows the energy resolution of each photopeak versus the corresponding photopeak centroid energy. Though this data series should be inversely proportional to the square root of the photopeak centroid energy [23], it more closely fits a trend of inverse proportionality to the photopeak centroid energy. The reason for this phenomenon will be investigated in future works.

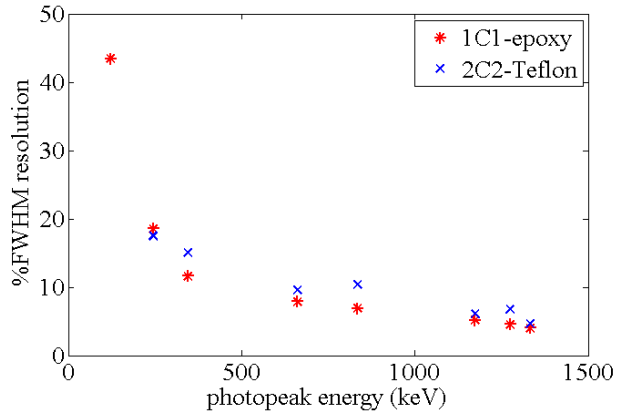

Fig. 7. Percent FWHM energy resolution versus energy, measured from the top 1 position.. No trend line was fit to either data series because they did not conform to the expected trend of inverse proportionality to energy. Error bars are within the size of the data points.

The best intrinsic photopeak efficiencies at 662 keV for assembly 1-$C1_{epoxy}$ were $8.95x10^{-3}$% and $3.65x10^{-3}$% from positions top2 and side2, respectively. Figure 8 shows the intrinsic photopeak efficiency of each of the gamma energy peaks for the spectrometer using assembly 1-$C1_{epoxy}$. As expected, the efficiency decreases as the photopeak energy increases.

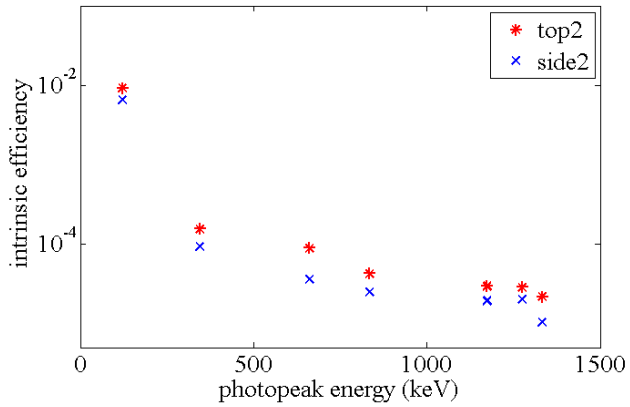

Fig. 8. Instrisic photopeak efficiencies for assembly 1- $C1_{epoxy}$ in the top2 and side2 positions. Error bars are within the size of the data points.

IV. Conclusion

A small prototype gamma spectrometer was developed using a SSPM coupled to a CsI(Tl) crystal and a FPGA-based DPP. It has achieved 7.88% FWHM energy resolution at 662 keV and an intrinsic efficiency of $8.95x10^{-5}$ at 257 mm from the top of the detector. Though the energy resolution at 662 keV is comparable to other published works, it is worse than the best known resolution.

The worse-than-expected energy resolution could be the result of a number of different individual factors or a combination of them. The light collection and reflection, inherent SSPM non-linearity, optimal bias voltage, preamplifier, and temperature may all have contributed. To construct an effective spectrometer with energy resolution closer to that of other works, these potential issues must be addressed.

The light collection and reflection must be better assessed in order to understand not only full resolution potential, but also to understand the true dynamic range and non-linearity of the combination of SSPM and CsI(Tl).

The optimal bias voltage and a charge-sensitive preamplifier will be implemented in future systems. These factors were overlooked in this study, and are expected to improve the energy resolution of the system.

Finally, thermal stabilization will be implemented in order to ensure no peak centroid drift in our system. However, since this system is meant to be the prototype for a mobile, rugged system, temperature correction, likely via FPGA firmware, will be implemented so that future versions will automatically adjust to changing temperatures and be able to operate effectively in different climates with no need for re-calibration.

Acknowledgment

E. M. Becker thanks S. Smith for assistance with the construction of the test stand and C. Seifert for her thoughts on this work.

REFERENCES

[1] D. Renker, "Geiger-mode avalanche photodiodes, history, properties, and problems," *Nucl. Instrum. Meth. A*, vol. 567, no. 4, pp. 48-56, Jun. 2006.

[2] P. Buzhan, *et. al.*, "An Advanced Study of Silicon Photomultiplier," *ICFA Instrumentation Bulletin*, vol. 23, 2002.

[3] "Introduction to the SPM", *SensL*, 2011. http://www.sensl.com

[4] A. Osovizky, "Scintillation Light Readout Using Silicon Photomultiplier – Review and Experimental Results", *Proc. Nuc. Sci. Symposium*, 2008, pp.2482-2483.

[5] M. Grodzicka, *et. al.*, "Energy resolution of scintillation detectors with SiPM light readout", *Proc. Nuc. Sci. Symposium*, 2010, pp.1940-1948.

[6] T Szczęśniak, *et al.*, "Characteristics of scintillation detectors based on inorganic scintillators and SiPM light readout", *Nuc. Instrum. Meth. A*, http://dx.doi.org/10/1016/j.nima/2012/09/011 (in press).

[7] G. Knoll, *Radiation Detection and Measurement*, 3rd ed. Hoboken, NY: John Wiley & Sons, 2000, pp. 398.

[8] DC Konnoff, "SSPM-based optical fiber radiation dosimeter", *Oregon State University*, Department of Nuclear Engineering and Radiation Health Physics, MS Thesis, 2012.

[9] WG Gong, *et al.*, "Resolution tests of CsI(Tl) scintillators read out by PIN diodes", *Nucl. Instrum. Meth. A*, vol. 268, no. 1, May 1988, pp. 190-199.

[10] "MicroSL Silicon Photomultiplier Detectors", *SensL* datasheet, 2011. http://www.sensl.com

[11] "Wrapping Scintillator Crystals to Optimize Light Collection", *SensL* product document, 2011. http://www.sensl.com

[12] "Wideband, Unity-Gain Stable, FET-Input Operational Amplifier", *Texas Instruments*, Dec. 2001. http://www.ti.com

[13] "Micro-EVB Preamp and Power Supply Molude for the MicroSL family of SPMs", *SensL*, 2011. http://www.sensl.com

[14] "RX1200 User's Manual", Avicenna Instruments, LLC, 2008.

[15] M Grodzicka, *et al.*, "2x2 MPPC arrays in gamma spectroscopy with CsI(Tl), LSO:Ce(Ca), $LaBr_3$, BGO", *2011 IEEE Nucl. Sci. Symposium Conference Record*, Oct 2011, pp. 1683-1692.

[16] AG Stewart, *et. al.*, "Performance of a 1-mm^2 silicon photomultiplier", *IEEE Journ. Quant. Electr.* vol. 44, no. 2, Feb. 2008, pp. 157-164.

[17] G. Knoll, *Radiation Detection and Measurement*, 3rd ed. Hoboken, NY: John Wiley & Sons, 2000, pp. 610-611.

[18] *IEEE Standard Test Procedures for Germanium Gamma-Ray Detectors*, ANSI/IEEE Standard 325, 1986.

[19] D. W. Aitken, et. al. "The Fluorescent Response of NaI(Tl), CsI(Tl), CsI(Na), and CaF2(Eu) to X-Rays and Low Energy Gamma Rays", *IEEE Trans. Nuc. Sci*., vol. 14, no. 1, Feb. 1967, pp. 468-477.

[20] A Syntfeld-Każuch, *et. al.*, "Non-Proportionality and Energy Resolution of CsI(Tl)", *IEEE Trans. Nuc. Sci.*, vol. 54, no. 5, Oct. 2007, pp. 1836-1841.

[21] V. Andreev, *et. al.*, "A high-granularity scintillator calorimeter readout with silicon photomultipliers", *Nuc. Instrum. Meth. A*, vol 540, Dec. 2004, pp.368-380.

[22] G. Knoll, *Radiation Detection and Measurement*, 3rd ed. Hoboken, NY: John Wiley & Sons, 2000, pp. 235.

[23] G. Knoll, *Radiation Detection and Measurement*, 3rd ed. Hoboken, NY: John Wiley & Sons, 2000, pp. 113-116.